One-bit Time Reversal for WLAN Applications

Persefoni Kyritsi and George Papanicolaou
Department of Mathematics
Stanford University
Stanford, CA 94305-2125
Email: kyritsi, papanico@math.stanford.edu

Abstract **Time reversal (TR) is a technique that can achieve remarkable temporal focusing (delay spread reduction) and spatial focusing (low spatial interference) in the context of wideband multiple/ single input-single output systems. In this paper, we investigate a simpli ed form of time-reversal, referred to as one-bit time reversal. The ef ciency of this technique has already been demonstrated for ultrasound applications. We apply it to radio waves and demonstrate that it can preserve the spatial focusing properties of TR, while requiring much simpler transmit lters. However, it does not have as good temporal focusing properties as pure TR.**

I. Introduction

Time reversal (TR) is a method to focus spatially and compress temporally broadband signals through a richly scattering environment [1], [2]. It involves two stages. In the first stage (channel estimation stage), a source emits a short pilot signal. This signal propagates and its response is recorded by each element of an array that will act as a transmitter in the data transmission stage. The duration of each of these recorded signals is significantly longer than the initial pilot pulse due to multiple scattering. The second stage is the actual data transmission. In this stage, all the elements of the transmitter array send the same data stream, and each one filters the signal to be transmitted through a *time-reversal lter i.e.* a filter that has a form similar to the signal recorded at that particular element during the channel estimation stage, reversed in time. These signals focus sharply in space and compress tightly in time at the source location.

Extensive laboratory TR experiments have shown this spatial focus and temporal compression across a broad range of settings in ultrasound experiments (see [3] and references contained within). Much research activity has been dedicated to using TR for multiple-input/single-output (MISO) underwater communication systems. In fact, several experiments in the ocean have demonstrated MISO-TR communications to be feasible [4]–[8].

Recently, there has been an effort to apply the principle of TR to electromagnetic waves at radio frequencies. The first experimental demonstration showed that indeed it is possible to achieve temporal compression of wideband signals that are transmitted over the radio channel [10]. A different experiment illustrated the spatial focusing properties of TR for electromagnetic waves using a narrowband system [9]. The post-processing of wideband fixed wireless access channel measurements showed that it is possible to reduce the delay spread of the channel, by using conventional TR or advanced weighting schemes [12], [13]. Moreover, post-processing of ultra wideband measurements illustrated the spatial focusing potential of a TR system that employs a single transmit antenna [21].

Temporal focusing is a desired property because it provides a method to reduce intersymbol interference (ISI). Hence, a TR communication system reduces the required complexity at the receiver. Spatial focusing on the intended receiver is also a desirable property because it indicates that the communications system has a low probability of intercept (LPI) by another receiver located nearby [15].

In this paper we study the advantages gained by TR communication, using standard TR and its simplified form, which is known as one-bit TR [24]. For our numerical simulations, we implement the 802.11n channel model that is applicable for systems with bandwidth up to 100MHz around either 2.5 or 5GHz.

The remainder of this paper is organized as follows. In Section II we discuss TR and one-bit TR. In Section III we discuss the channel model that is used for our simulations. Section IV shows the results of the simulations, and the conclusions are in Section V.

II. System Description

A. Fundamentals of TR Systems

We describe the operation of a downlink TR system with N_{TX} transmit antennas as a two-stage process. In the following we denote as $h(t; \underline{r}_{TX}, \underline{r}_{RX})$ the channel impulse response from a transmitter at location $\underline{r}_{TX}$ to a receiver at location $\underline{r}_{RX}$.

1) Channel estimation: The first stage is the channel estimation stage, during which each element of the transmit array obtains knowledge of the channel impulse response to the intended receiver. There are several ways in which channel estimation can be implemented (*e.g.* with a pilot signal sent by the intended receiver, or with feedback of CSI to the transmitter), which make them more or less suitable for FDD/ TDD systems. In any case, the accuracy of the CSI at the transmitter depends on the implementation details, the noise during that process, its repetition rate and the rate of change of the channel. In this paper, we are not concerned with the specifics of the channel estimation and assume that the transmitter has perfect and instantaneous CSI.

978-3-8007-2909-8/05/$20.00 ©2005 IEEE

2) Data transmission: The second stage is the actual data transmission. The Tx uses the CSI it acquired during the channel estimation stage to transmit a bitstream: each of the N_{TX} elements of the transmit array transmits simultaneously the same signal $x(t)$, by filtering it through a filter $g(t)$. If the signal to be transmitted is $x(t)$, then the received signal at the Rx is $y(t)$ and can be written as

$$y(t) = \sum_{m=1}^{N_{Tx}} h(t; \underline{r}_{TX_m}, \underline{r}_{RX}) \otimes g_m(t; \underline{r}_{Txm}, \underline{r}_{RX}) \otimes x(t) \quad (1)$$

$\otimes$ denotes the convolution operator. The equivalent channel impulse response is given as

$$h_{eq}(t) = \sum_{m=1}^{N_{Tx}} h(t; \underline{r}_{TX_m}, \underline{r}_{RX}) \otimes g_m(t; \underline{r}_{TX_m}, \underline{r}_{RX}). \quad (2)$$

When $N_{TX} = 1$, we refer to the transmission scheme as SISO TR, whereas when $N_{TX} > 1$, we refer to the transmission scheme as MISO TR.

In pure TR, the filter $g_m(t)$ at the m-th transmit antenna is the time reversed and phase conjugated version of the channel impulse response to the intended receiver.

$$g_m^{TR}(t) = h\ (-t; \underline{r}_{TX_m}, \underline{r}_{RX}) \quad (3)$$

$(\cdot)$ denotes the complex conjugate of the argument $(\cdot)$. $\underline{r}_{TX_m}$ is the location of the m-th transmit antenna. The equivalent channel impulse response in the case of pure TR is given as the sum of the autocorrelations of the channel impulse responses to the individual array elements. Therefore it is symmetric around $t = 0$, and it achieves its maximum at $t = 0$. This determines the synchronization between Tx and Rx, as well as the sampling time at the Rx.

One-bit TR is a simplified form of the transmit filter $g_m(t)$ [24]. Namely

$$\begin{array}{c} g_m^{one-bitTR}(t) = \\ sgn(Re\ \ h(-t; \underline{r}_{TX_m}, \underline{r}_{RX})\ \ ) \\ -jsgn(Im\ \ h(-t; \underline{r}_{TX_m}, \underline{r}_{RX})\ \ ) \end{array} \quad (4)$$

The transmit filters in one-bit TR preserve only the sign information of the real and imaginary parts of the channel impulse response. Equivalently, they only retain the phase information of the channel impulse response. The most important advantages of these filters compared to pure TR filters are: a) One bit TR filters are simpler to implement in digital form, b) If the system relies of feedback of CSI to the transmitter, the required amount of information feedback is much more limited ($2L$ bits per transmit antenna would need to be fed back, instead of $2L \times A$, where A is the number of bits required to represent a number with the desired accuracy), c) One-bit TR is expected to be less sensitive to channel estimation errors, and d) The transmit power is strictly controlled, and does not vary from antenna to antenna.

Both types of TR filters double the temporal extent of the channel. Pure TR in a SISO situation does not reduce the perceived delay spread of the channel [14]. It can do so in a MISO scenario due to the incoherent addition of the responses from the various transmit elements at delays $\tau \neq 0$.

The underlying assumption is that the channel transfer functions have not changed in the data transmission stage relative to the channel estimation stage.

B. Temporal focusing

The common measure for the temporal extent of the channel impulse response is the delay spread (DS), which is defined as the second central moment of the channel power delay profile $pdp(\tau)$:

$$DS^2 = \frac{1}{\int_{-\infty}^{+\infty} pdp(\tau)d\tau} \int_{-\infty}^{+\infty} (\tau - \bar{\tau})^2\, pdp(\tau)d\tau \quad (5)$$

where

$$pdp(\tau) = E\left[|h(\tau)|^2\right] \quad (6)$$

$$\bar{\tau} = \frac{1}{\int_{-\infty}^{+\infty} pdp(\tau)d\tau} \int_{-\infty}^{+\infty} \tau pdp(\tau)d\tau \quad (7)$$

The power delay profile is calculated as the expected value of the power of the channel impulse response within the local area of the transmitter/ receiver. Large delay spread leads to irreducible bit error rate (BER), and is therefore a fundamental limitation for wireless systems [18].

We investigate the perceived delay spread that can be achieved after the application of TR and one-bit TR at the transmitter, by applying the above calculation to the corresponding equivalent channel impulse responses.

C. Spatial Focusing

Let us assume that the system performs TR with a view to communicating with an intended receiver that is located at $\underline{r}_{RX}$. We are interested in the amount of interference this operation causes at a location at distance $\underline{d}$ away from the intended receiver, *i.e.* at a location $\underline{r}' = \underline{r}_{RX} + \underline{d}$.

Low interference power at location $\underline{r}'$ would mean that it would be possible to simultaneously send data to both locations $\underline{r}$ and $\underline{r}'$, without impairing each individual communications link. Alternatively, the received power away from the target is a measure of the system's probability of intercept: low power at a distance $\underline{d}$ away from the intended receiver indicates that an eavesdropper at that location would not be able to successfully intercept the content of the communication.

The equivalent channel impulse response at location $\underline{r}'$ is given as

$$h_{eq}(t; \underline{r}') = \sum_{m=1}^{N_{Tx}} h(t; \underline{r}_{TX_m}, \underline{r}') \otimes g_m(t) \quad (8)$$

where $h(t; \underline{r}_{TX_m}, \underline{r}')$ indicates the channel impulse response from the m-th transmitter to $\underline{r}'$.

Assuming a perfectly synchronous system, and keeping in mind that the the equivalent channel impulse response on the intended receiver in pure TR achieves its maximum at $\tau = 0$, we concentrate on the value of the interference at that sampling instant:

$$IF(\underline{r}') = h_{eq}(0; \underline{r}') \quad (9)$$

III. CHANNEL MODEL

In the following, we give a brief description of the principles that underlie the 802.11n channel model, which will be used for our simulations. Details can be found in [19].

A. Tap delay line model

The channel impulse response of a wideband system can be expressed as a tap delay line model with L taps of the form

$$h(\tau) = \sum_{l=0}^{L-1} h_l \delta(\tau - \tau_l) \quad (10)$$

The l-th tap has complex amplitude h_l and arrives at delay τ_l. The tap amplitudes follow a known power delay profile pdp

$$E[|h_l|^2] = pdp(\tau_l) = P_l \quad (11)$$

The statistical distribution of the tap amplitudes depends on the propagation conditions. In this paper we assume that the amplitudes h_l are Rayleigh distributed.

B. Correlation and power azimuth spectrum

The cross-correlation between the waves impinging on two antenna elements has been studied in various references, and it has been shown to be a function of the Power Azimuth Spectrum (PAS) and the radiation pattern of the antenna elements. Antenna elements will be assumed to be omnidirectional in the following.

We define the random variables $x = x_I + j \cdot x_Q = h_l(\mathbf{r}), y = y_I + j \cdot y_Q = h_l(\mathbf{r} + \mathbf{d})$. x, y denote the complex amplitude of the l-th tap at locations $\mathbf{r}$ and $\mathbf{r}' = \mathbf{r} + \mathbf{d}$ respectively. x_I, y_I denote the in phase components of x, y respectively, and x_Q, y_Q denote the quadrature components of x, y respectively.

For Rayleigh channels, it can easily be shown that the following properties hold for the correlations of x_I, y_I, x_Q, y_Q [17]:

$$R_{x_I y_I} = R_{x_Q y_Q}, R_{x_I y_Q} = -R_{x_Q y_I} \quad (12)$$

The complex correlation of x, y is given by $\rho = R_{x_I y_I} + jR_{x_I y_Q}$.

The correlations depend on the power azimuth spectrum according to the following equations:

$$R_{x_I y_I}(\mathbf{d}) = \int_+^- cos\left(kd\cos(\phi - \theta)\right) PAS\left(\phi\right) d\phi, \quad (13)$$

$$R_{x_Q y_I}(\mathbf{d}) = \int_+^- sin\left(kd\sin(\phi - \theta)\right) PAS\left(\phi\right) d\phi \quad (14)$$

The incidence vector $\mathbf{k}$ is defined for a wave impinging from the azimuth direction ϕ, as $\mathbf{k} = \frac{2}{\lambda}\left(cos\phi\hat{x} + sin\phi\hat{y}\right)$, and $\mathbf{d} = d\left(cos\theta\hat{x} + sin\theta\hat{y}\right)$ ($\hat{x}$, $\hat{y}$ are the unitary vectors along the x and y directions respectively).

In the limiting case of uniform PAS over $[0, 2\ ]$, the correlation is the well-known zero-th order Bessel function of the first kind. In the more general case, the PAS is characterized by its shape and clustering characteristics. The parameters of interest are in that case the Angle of Arrival (AoA) and Angular Spread (AS-Rx) around the receiver, and the Angle of Departure (AoD) and Angular Spread around the transmitter (AS-Tx).

C. Kronecker model

Let $u = h_l(\underline{r}_{TX_m}, \underline{r}_{RX_p})$ be the complex amplitude of the l-th tap of $h(\tau; \underline{r}_{TX_m}, \underline{r}_{RX_p})$. Similarly $v = h_l(\underline{r}_{TX_n}, \underline{r}_{RX_q})$ is the complex amplitude of the l-th tap of $h(\tau; \underline{r}_{TX_n}, \underline{r}_{RX_q})$.

The 802.11n channel model assumes the Kronecker property for the channel correlation, *i.e.* it assumes that the correlation on the transmitting and the receiving sides are separable [16]:

$$\rho(u, v) = \rho_{RX}(\underline{r}_p - \underline{r}_q) \cdot \rho_{TX}(\underline{r}_m - \underline{r}_n) \quad (15)$$

$\rho_{RX}(\underline{r}_p - \underline{r}_q)$ is the receive correlation which involves only the locations of the receivers p, q, and $\rho_{TX}(\underline{r}_m - \underline{r}_n)$ is the transmit correlation which involves only the locations of the transmitters m, n. These can be calculated from the PAS around the receiver/ transmitter location respectively.

D. The 802.11n channel model

[19] describes a set of 2-dimensional 802.11n channel models applicable to indoor MIMO wireless local area network (WLAN) systems. The 802.11n channel models are based on the cluster model developed by Saleh and Valenzuela ([22]), whereby channel taps arrive clustered in time. The new models also display clustering in angle, a property that has been experimentally demonstrated in various environments (see [23] among others).

The model can be used for both $2GHz$ and $5GHz$ frequency bands. The minimum tap spacing in all the models is $T_u = 10ns$. Although the systems that the 802.11n channel models address have a bandwidth $B_{802.11n} = 20MHz$, we can use the model to characterize bandwidths up to $1/T_u = 100MHz$.

In total, there are 6 channel models that correspond to different types of propagation scenarios. Specifically we use Model B that corresponds to the environment of a residential building or a small office. Fig. 1 shows the tap delay line model for this scenario (not normalized to unit total power). The delay spread is about $15ns$, and we can clearly distinguish two clusters by visual inspection of the tap delay line. The cluster parameters are summarized in Table I.

The simulations developed in this paper are based on the the software that accompanies the channel model (details can be found in [20]). Since we are interested in the field in a local area around the intended receiver, we look at a grid of points around the target and place fictitious receive antennas at each point of the grid. The implication is that the size of the computational problem increases significantly.

TABLE I
ANGULAR PARAMETERS FOR MODEL B

Cluster	1	2
Mean AoA	4.3^o	118.4^o
AS (Rx)	14.4^o	25.2^o
Mean AoD	225.1^o	106.5^o
AS (Tx)	14.4^o	25.4^o

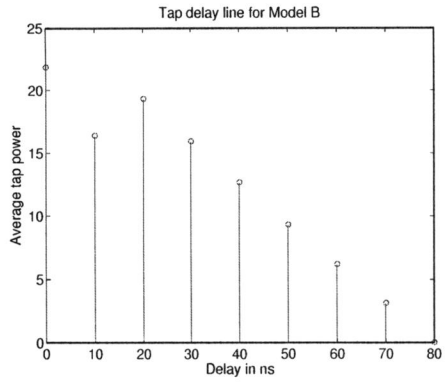

Fig. 1. Tap delay line for Model B

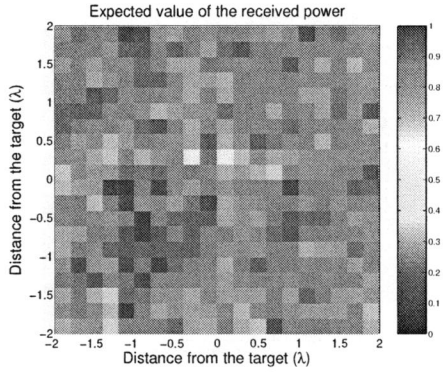

Fig. 2. Spatial focusing in the baseline scenario

IV. Temporal and Spatial Focusing

We look at the average over 100 realizations of a channel that follows the description of the 802.11n channel model B.

A. Delay spread reduction

Table II shows the delay spread for the communication scenarios under investigation. The delay spread of the original channel is $15.65ns$. The DS predicted by the simulation is very close to its theoretical estimate. With pure TR in a SISO situation the DS of the channel is not reduced. The application of pure TR from multiple antennas aids in the reduction of the DS. One-bit TR results in DS higher than that of the original channel, however its performance is also improved with the addition of more transmit antennas.

B. Spatial focusing analysis

In the absence of pre-processing at the transmitter, each receiver performs a matched filtering operation with the corresponding filter $h(t;\underline{r})$ in order to detect the transmitted signal. Clearly no spatial focusing can be achieved as shown in Fig 2: all locations achieve about the same amount of power.

Fig. 3 shows the expected value of the interference power in an area 4×4 around the intended receiver, assuming that the transmitter applies pure TR or one-bit TR. The power off the target has been normalized by the average peak received power on the target.

The comparison with Fig 2 clearly demonstrates the spatial focusing benefits of TR. The spatial focusing is not omni-directional, because of the directional characteristics of the clusters. Indeed, it can easily be shown that in situations of varied cluster mean angles of arrival, the spatial interference pattern is more uniform. Nonetheless at distances 2 away from the intended receiver, the expected received power is more than $5dB$ lower than the expected power on the target. One-bit TR retains this property.

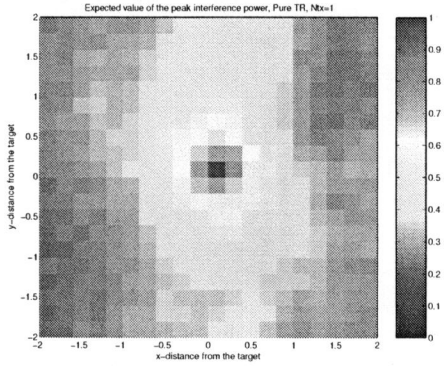

(a) Pure TR

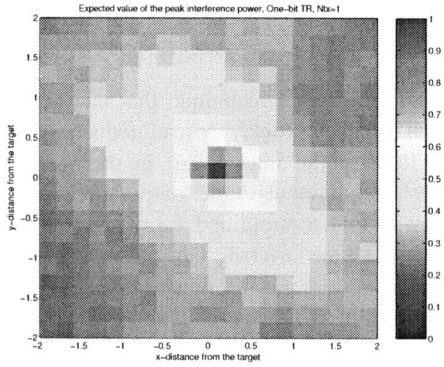

(b) One-bit TR

Fig. 3. Comparison of (a) pure TR, and (b) 1-bit TR, in a SISO situation

We now look at the effect of increasing the number of transmit antennas, assuming uncorrelated transmitters. Fig. 4 shows the spatial focusing performance when $N_{TX} = 2$.

The comparison of Fig. 3 with Fig. 4 shows that indeed spatial focusing improves with the introduction of more transmit elements. Indeed the expected received power falls at the level of more than $5dB$ lower than the expected power on the target at distances of 1 , if 2 transmitters are employed.

TABLE II
Delay spread comparison for a Model B channel

No TR		$16.04ns$
Pure TR	$N_{TX} = 1$	$16.43ns$
	$N_{TX} = 2$	$13.16ns$
One-bit TR	$N_{TX} = 1$	$28.02ns$
	$N_{TX} = 2$	$25.37ns$

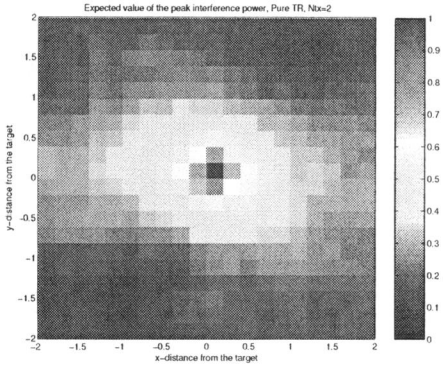

(a) Pure TR

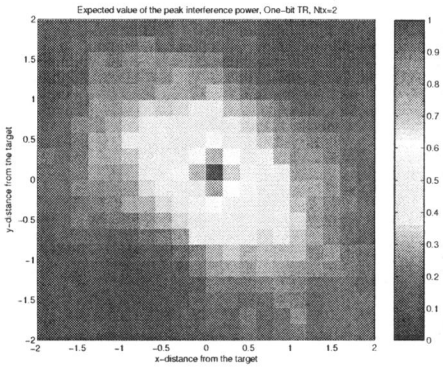

(b) One-bit TR

Fig. 4. Comparison of (a) pure TR, and (b) 1-bit TR, in a MISO situation

V. Conclusion

Time reversal is a technique that can achieve remarkable temporal focusing (delay spread reduction) and spatial focusing (low spatial interferece) in the context of wideband multiple/ single input-single output systems. In this paper, we showed that a simplified form of time-reversal, referred to as one-bit time reversal, can preserve the spatial focusing properties, while requiring much simpler transmit filters. The disadvantage of this approach is that it increases the perceived delay spread of the channel. If the receivers have advanced equalization capabilities, this factor is not expected to limit their performance, whereas the system can benefit from the low spatial interference, either for multi-user or low probability of intercept considerations.

Acknowledgment

This work of was supported partially by grants NSF: DMS-0354674-001 and ONR: N00014-02-1-0088.

References

[1] M. Fink, "Time reversed acoustics," *Physics Today*, March, pp. 33-40, 1997.

[2] M. Fink, "Time-reversed acoustics," *Scientific American*, November, pp. 91-97, 1999.

[3] M. Fink, D. Cassereau, A. Derode, C. Prada, P. Roux, M. Tanter, J-L. Thomas and F. Wu, "Time-reversed acoustics," *Reports on Progress in Physics*, vol. 63, pp. 1933-1995, 2000.

[4] W. A. Kuperman, W. S. Hodgkiss, H. C. Song, T. Akal, C. Ferla, and D. R. Jackson, "Phase conjugation in the ocean: Experimental demonstration of a time reversal mirror," *J. Acoust. Soc. Am.*, vol. 103, pp. 25-40, 1998.

[5] W. S. Hodgkiss, H. C. Song, W. A. Kuperman, T. Akal, C. Ferla and D. R. Jackson, "A long-range and variable focus phase-conjugation experiment in shallow water," *J. Acoust. Soc. Am.*, vol. 105, pp. 1597-1604, 1999.

[6] S. Kim, G. Edelmann, W. S. Hodgkiss, W. A. Kuperman, H. C. Song, and T. Akal, "Spatial resolution of time reversal array in shallow water," *J. Acoust. Soc. Am.*, vol. 110, pp. 820-829, 2001.

[7] G. Edelmann, T. Akal, W. S. Hodgkiss, S. Kim, W. A. Kuperman, H. C. Song, "An initial demonstration underwater acoustic communication using time reversal," *IEEE J. of Oceanic Eng.*, vol. 27, pp. 602-609, 2002.

[8] S. Kim, W. A. Kuperman, W. S. Hodgkiss, H. C. Song, G. Edelmann, and T. Akal, "Robust time reversal focusing in the ocean," *J. Acoust. Soc. Am.*, vol. 114, pp. 145-157, 2003.

[9] B.E. Henty, D.D. Stancil, "Multipath-enabled super-resolution for rf and microwave communications using phase-conjugate arrays," in *Physical Review Letters*, no 93, December 2004.

[10] G. Lerosey, J. de Rosny, A. Tourin, A. Derode, G. Montaldo, and M. Fink, "Time Reversal of electromagnetic waves," in *Physical Review Letters*, no 92, 2004.

[11] C. Oestges, A. D. Kim, G. Papanicolaou, A. J. Paulraj, "Characterization of space-time focusing in time-reversed random fields," *IEEE Trans. Antennas and Propagation.*, Jan. 2005, vol. 53 , no 1, pp. 283-293.

[12] P. Kyritsi, G. Papanicolaou, P. Eggers and A. Opera, "MISO time reversal and delay spread compression for FWA channels at 5 GHz," *Antennas and Wireless Propagation Letters* vol. 3, pp. 96-99, 2004.

[13] P. Kyritsi, G. Papanicolaou, P. Eggers, and A. Oprea, "Time reversal techniques for wireless communications," in *Proc. IEEE 60th Vehicular Technology Conference*, Sept. 2004.

[14] P. Kyritsi, and G. Papanicolaou, "Time-Reversal: Spatio-temporal focusing and its dependence on the channel properties," submitted for publication in *IEEE Trans. on Antennas and Propagation.*

[15] A. Kim, P. Kyritsi, P. Blomgren, and G. Papanicolaou, "Low probability of intercept and intersymbol interference in multiple-input/ single-output time reversal communication systems," submitted to *IEEE Journal of Oceanic Engineering*, Nov. 2004.

[16] J.P. Kermoal, L. Schumacher, K.I. Pedersen, P.E. Mogensen, and F. Frederiksen, "A stochastic MIMO radio channel model with experimental validation," *IEEE Journal on Selected Areas in Communications*, vol. 20 , no 6, pp. 1211-1226, Aug. 2002.

[17] L. Schumacher, K.I. Pedersen, and P.E. Mogensen, "From antenna spacings to theoretical capacities - guidelines for simulating MIMO systems," in Proc. 13th IEEE International Symposium on Personal, Indoor and Mobile Radio Communications, 2002, vol. 2, pp. 587-592.

[18] J. Chuang, "The Effects of Time Delay Spread on Portable Radio Communications Channels with Digital Modulation," in *IEEE Journal on Selected Areas in Communications*, Vol. 5, no. 5, June 1987, pp. 879 -889.

[19] V. Erceg, L. Schumacher, P. Kyritsi, A. Molisch, D.S. Baum, et al. "TGn channel models," IEEE 802.11-03/940r2, Jan. 2004.

[20] L. Schumacher, and B. Dijkstra, "Description of a MATLAB implementattion of the indoor MIMO WLAN channel model proposed by the IEEE 802.11 TGn channel model special committee", ftp://ieee:wireless@ftp.802wirelessworld.com/11/03/11-03-0940-04-000n-tgn-channel-models.doc

[21] M. Emami, J. Hansen, A.D. Kim, G. Papanicolaou, A.J. Paulraj, D. Cheung, and C. Prettie, "Predicted Time Reversal Performance in Wireless Communications Using Channel Measurements," accepted for publication in *IEEE Communications Letters.*

[22] A.A.M. Saleh and R.A. Valenzuela, "A statistical model for indoor multipath propagation," in *IEEE J. Select. Areas Commun.*, vol. 5, 1987, pp. 128-137.

[23] Chia-Chin Chong, D.I. Laurenson and S. McLaughlin, "Statistical Characterization of the 5.2 GHz wideband directional indoor propagation channels with clustering and correlation properties," in Proc. IEEE Veh. Technol. Conf., vol. 1, Sept. 2002, pp. 629-633.

[24] A. Derode, A. Tourin, M. Fink, "Ultrasonic pulse compression with one-bit time reversal through multiple scattering," in J. Acoust. Soc. Am. 85, 1999, vol. (9), pp. 6343-6352.